

Retrieval of convective boundary layer wind field statistics from radar profiler measurements in conjunction with large eddy simulation

DANNY SCIPIÓN^{*1,3}, ROBERT PALMER^{2,3}, PHILLIP CHILSON^{2,3}, EVGENI FEDOROVICH² and AARON BOTNICK²

¹School of Electrical and Computer Engineering, University of Oklahoma, Norman, USA

²School of Meteorology, University of Oklahoma, Norman, USA

³Atmospheric Radar Research Center, University of Oklahoma, Norman, USA

(Manuscript received October 10, 2008; in revised form January 23, 2009; accepted February 23, 2009)

Abstract

The daytime convective boundary layer (CBL) is characterized by strong turbulence that is primarily forced by buoyancy transport from the heated underlying surface. The present study focuses on an example of flow structure of the CBL as observed in the U.S. Great Plains on June 8, 2007. The considered CBL flow has been reproduced using a numerical large eddy simulation (LES), sampled with an LES-based virtual boundary layer radar (BLR), and probed with an actual operational radar profiler. The LES-generated CBL flow data are then ingested by the virtual BLR and treated as a proxy for prevailing atmospheric conditions. The mean flow and turbulence parameters retrieved via each technique (actual radar profiler, virtual BLR, and LES) have been cross-analyzed and reasonable agreement was found between the CBL wind parameters obtained from the LES and those measured by the actual radar. Averaged vertical velocity variance estimates from the virtual and actual BLRs were compared with estimates calculated from the LES for different periods of time. There is good agreement in the estimates from all three sources. Also, values of the vertical velocity skewness retrieved by all three techniques have been inter-compared as a function of height for different stages of the CBL evolution, showing fair agreement with each other. All three retrievals contain positively skewed vertical velocity structure throughout the main portion of the CBL. Radar estimates of the turbulence kinetic energy (eddy) dissipation rate (ϵ) have been obtained based on the Doppler spectral width of the returned signal for the vertical radar beam. The radar estimates were averaged over time in the same fashion as the LES output data. The agreement between estimates was generally good, especially within the mixing layer. Discrepancies observed above the inversion layer may be explained by a weak turbulence signal in particular flow configurations. The virtual BLR produces voltage measurements consistent with the LES data fields. First-, second-, and third-order statistics (mean wind, variance, and skewness) of vertical velocity obtained from BLR output demonstrate its suitability for validating radar-profiler signal processing algorithms.

Zusammenfassung

Die konvektive Grenzschicht (convective boundary layer, CBL) der Atmosphäre ist am Tag durch starke Turbulenz gekennzeichnet, welche hauptsächlich durch den Auftrieb der an der Erdoberfläche erwärmten Luftmassen hervorgerufen wird. Diese Studie befasst sich mit einem Beispiel der Strömungsstrukturen der konvektiven Grenzschicht, wie sie in den Great Plains (USA) am 8. Juni 2007 beobachtet wurden. Die konvektive Grenzschicht an diesem Tag wurde numerisch mit einer Large Eddy Simulation (LES) reproduziert, mittels eines auf LES basierenden Grenzschicht-Radars (boundary layer radar, BLR) untersucht, und mit einem operativen Wind-Profil Radar gemessen. Die LES Ergebnisse für die konvektive Strömung werden dabei in das virtuelle Grenzschicht-Radar als Ersatz für die vorherrschenden, atmosphärischen Bedingungen eingelesen und bearbeitet. Die mittlere Strömung und die Turbulenzparameter, die mit der jeweiligen Technik (reales Wind-Profil Radar, virtuelles BRL, und LES) ermittelt wurden, wurden verglichen. Die LES-Ergebnisse für die mittlere Strömung der konvektiven Grenzschicht stimmen gut mit den Messdaten des Wind-Profil Radars überein. Für die mittlere Varianz der vertikalen Geschwindigkeit zu verschiedenen Zeiten wurden aus den Daten des Wind-Profil Radars und des virtuellen BLRs ebenfalls ähnliche Werte wie für die LES-Berechnungen ermittelt. Außerdem wurde die mit allen drei Methoden berechnete Schiefe der vertikalen Geschwindigkeitskomponente als Funktion der Höhe für verschiedene Zeitintervalle der CBL-Entwicklung verglichen. Auch hier wurde eine gute Übereinstimmung der Werte gefunden, und alle drei Methoden ergaben eine positive Schiefe für den Hauptteil der CBL. Radarabschätzungen der turbulenten kinetischen Energiedissipationsrate ϵ wurden aus der Breite des Dopplerspektrums des zurückgestreuten Signals des vertikalen Radarstrahls ermittelt. Die Radarabschätzungen für ϵ wurden auf die gleiche Weise wie die LES-Daten über einen bestimmten Zeitraum gemittelt. Die Übereinstimmungen zwischen den ϵ -Werten waren generell gut, besonders innerhalb der Mischungsschicht. Die Abweichungen, die oberhalb der Inversionsschicht beobachtet wurden, könnten durch ein schwaches Turbulenzsignal in bestimmten Strömungskonfigurationen erklärt werden. Das virtuelle BLR produziert Ergebnisse, die mit den LES Datafeldern konsistent sind. Algorithmen für die Signalverarbeitung eines Wind-Profil Radars können mit den Statistiken erster, zweiter, und dritter Ordnung (Mittelwert, Varianz, und Schiefe) der vertikalen Geschwindigkeit, die von dem virtuellen BLR ausgegeben werden, evaluiert werden.

*Corresponding author: Danny Scipión, University of Oklahoma, School of Meteorology, 120 David L. Boren Blvd., Rm 5900, Norman, OK 73072-7307, USA, e-mail: dscipion@ou.edu

1 Introduction

Radar wind profilers are commonly used to obtain information regarding flow structure in atmospheric boundary layer flows. In SCIPION et al. (2007), a virtual radar profiler was applied to retrieve the three-dimensional wind field parameters for an atmospheric convective boundary layer (CBL) flow reproduced by means of numerical large eddy simulation (LES). In this experiment, five virtual boundary layer radars (BLRs) were equidistantly spaced within the LES domain and were directed at sampling volumes located at different heights within and above the CBL. Velocity values were obtained at each height with one-minute increments and were further used to evaluate wind parameters. The obtained estimates showed satisfactory agreement with the LES data. However, the configuration of five radars, as considered in SCIPION et al. (2007), was unrealistic when compared with normal operational settings.

A more conventional setup discussed in the present study is realized through the use of a single radar pointing in five non-coplanar directions. Also, a more realistic CBL case is considered incorporating typical forcings that drive a daytime clear CBL (BOTNICK and FEDOROVICH, 2008). Flow structure for this CBL case is investigated through both real radar measurements and numerical simulations. Numerically generated CBL flow fields are employed in two ways. First, they are used to emulate a virtual boundary layer radar (BLR) along the lines discussed in MUSCHINSKI et al. (1999) and SCIPION et al. (2008). Second, they represent a source of reference information about the CBL turbulent flow. In both virtual and real radar applications, the three wind components are obtained through application of the Doppler beam swinging (DBS) technique (BALSLEY and GAGE, 1982).

Mean flow and turbulence parameters retrieved by means of each technique (actual radar, virtual BLR, and LES) are analyzed in conjunction. Turbulence characteristics are investigated from the second- (SCIPION et al., 2007) and third-order statistics (MOENG and ROTUNNO, 1990) of the vertical velocity. The skewness (third-order statistics) is of importance for many applied CBL studies such as investigations of pollutant dispersion in the CBL. The Doppler spectral width of radial velocity has been evaluated as a basis for the retrieval of velocity component variances within the radar resolution volume (SPIZZICHINO, 1975; HOCKING, 1983, 1985, 1996; GOSSARD et al., 1990; COHN, 1995; WHITE, 1997; WHITE et al., 1999; GOSSARD et al., 1998; JACOBY-KOALY et al., 2002; SHAW and LEMONE, 2003). Different atmospheric processes contribute to the distribution of radial velocities within the resolution volume and affect, in turn, the Doppler spectral shape and width. Some of these processes lead to the broadening of the spectra and others, like the ground clutter removal algorithm (JACOBY-KOALY et al., 2002), to its narrowing. Only after removing all

external contributing factors, may one assume the remaining spectral width to be only due to turbulence. The residual spectral width is used to estimate the turbulence kinetic energy (eddy) dissipation rate (ϵ).

This paper is organized as follows. In Section 2, the main features of the LES code employed in this study are briefly described with a focus on recently implemented features and methodologies of using LES for CBL flow data generation. The virtual radar is presented in Section 3 along with the radar experimental setup. Section 4 discusses comparisons of wind fields and turbulence parameters obtained by different methods. Finally, in Section 5, conclusions are summarized and directions of future work are outlined.

2 Large eddy simulation

The main features of the LES code employed in our study are described by FEDOROVICH et al. (2004a,b) and CONZEMIUS and FEDOROVICH (2006). This code was extensively tested in comparison with several other representative LES codes and with experimental data for clear CBLs with and without wind shear (FEDOROVICH et al., 2004a; FEDOROVICH and CONZEMIUS, 2008). The code was found to confidently reproduce turbulence structure for a broad variety of flow regimes observed in the clear CBL. Over the last two years, the code has undergone several revisions aimed at improving its numerical accuracy and ability to perform in realistic atmospheric environments. For example, the formerly used leapfrog time advancement scheme with a weak filter was replaced by the Runge-Kutta third-order scheme (DURRAN, 1999). Simulation initialization procedures were modified to incorporate realistic atmospheric sounding data retrieved from observations or from larger-scale atmospheric model/analysis outputs (BOTNICK and FEDOROVICH, 2008).

The simulation for the present study has been performed in a rectangular domain composed of 20 m grid cells. The domain size is $X \times Y \times Z = 5.12 \times 5.12 \times 3.0 \text{ km}^3$. Correspondingly, the domain consists of $256 \times 256 \times 150$ grid elements. The time discretization was set to 1 s. Following the established LES methodology adopted in atmospheric and engineering turbulence studies, motions in the simulated turbulent CBL flow are subdivided into the larger-scale resolved motions, which are directly reproduced on the computational grid, and the smaller-scale, the so-called sub-grid motions, which are modeled through additional stress/flux terms in the discretized governing equations for the resolved quantities. The sub-grid stress and buoyancy flux are parameterized in terms of an eddy viscosity/diffusivity model based on an evolution equation for the sub-grid turbulence kinetic energy (TKE). The spatial discretization on the computational grid is of the second order in space. Enforcement of mass conservation in the simulated flow is realized by the pressure. A Poisson equation for pressure is constructed by combining the continuity and

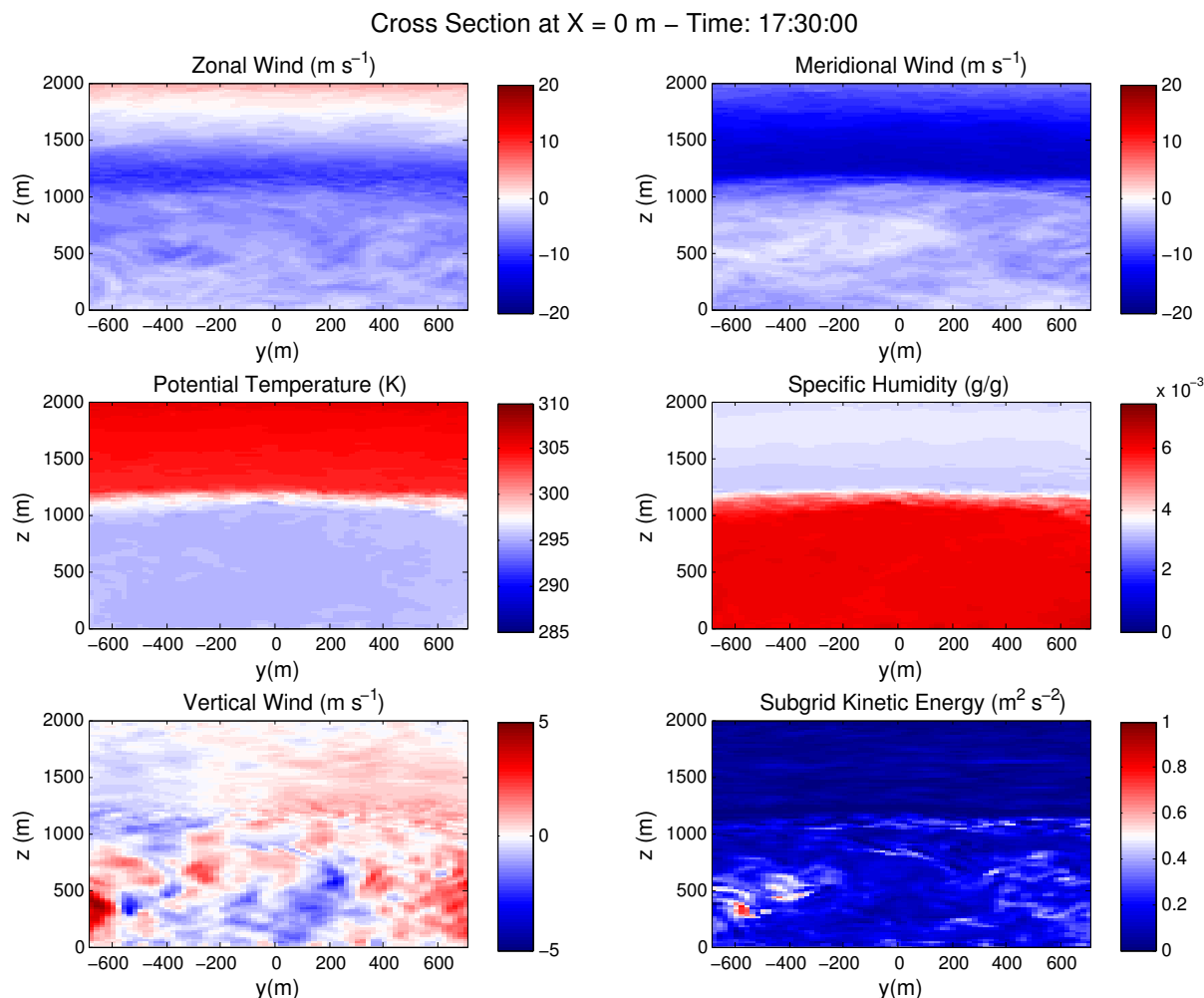


Figure 1: Examples of LES fields in the virtual radar sub-domain. Top-left: zonal wind. Top-right: meridional wind. Middle-left: potential temperature. Middle-right: specific humidity. Bottom-left: vertical wind. Bottom-right: sub-grid kinetic energy. All data presented refer to the same single realization in time.

momentum balance equations. The Poisson equation is solved numerically by the fast transform technique over horizontal planes, and by tri-diagonal matrix decomposition in the vertical. At the side-walls of the simulation domain, periodic boundary conditions are prescribed for prognostic variables (velocity components, potential temperature, specific humidity, and sub-grid TKE). In the upper 20 % fraction of the domain, a sponge layer is introduced in order to damp vertical motions close to the domain top and to ensure steady-state conditions at the upper boundary. To minimize the inevitable spurious influence of the sponge layer on the numerical solution, the time advancement is maintained only as long as the CBL depth is less than 70 % of the domain height. The no-slip boundary condition for velocity and zero-gradient condition for sub-grid energy are prescribed at the heated bottom surface. Monin-Obukhov similarity relationships are used point by point to couple local buoyancy and mechanical turbulence forcing within the lowest layer of grid cells. The surface roughness length,

temperature, and moisture fluxes are prescribed as external parameters.

The LES was applied to reproduce a daytime CBL case observed at the Southern Great Plains Atmospheric Radiation Measurement Climate Research Facility (SGP ACRF) in Lamont, Oklahoma, on June 8 2007. The LES setup for this case is described in BOTNICK and FEDOROVICH (2008). The LES output included instantaneous fields of the filtered flow velocity components, potential temperature and specific humidity, and the sub-grid TKE available with one-second time increments in the BLR sub-domain (see below). Also included in the output were flow statistics obtained locally, by temporal averaging, and spatial statistics obtained through averaging over horizontal planes. Spatial statistics have been evaluated throughout the duration of the run (about 12 hours) and over the whole domain. Evaluated statistics included mean flow variables, velocity, temperature, and humidity variances (both resolved and sub-grid), vertical fluxes of momentum, heat and moisture, and third-order

moments of the resolved vertical velocity and temperature fields.

A sub-set of the LES output was employed as an input data-set for the virtual BLR. The BLR sub-domain had spatial limits of $1860 \text{ m} \leq X \leq 3260 \text{ m}$, $1860 \text{ m} \leq Y \leq 3260 \text{ m}$, and $0 \text{ m} \leq Z \leq 2000 \text{ m}$. The BLR used three-dimensional fields of potential temperature Θ , specific humidity q , flow velocity components u , v , and w along the coordinate directions x , y , and z , respectively, and sub-grid TKE E . A snapshot of the simulated CBL flow structure is given in Figure 1. The presented instantaneous flow fields illustrate the main features of the CBL turbulent flow structure. By its nature, the clear atmospheric CBL is a turbulent boundary layer, whose turbulence is primarily forced by heating from the underlying surface. One may see an intensive turbulent mixing of momentum and scalar fields in the main portion of the CBL, beneath the so-called capping inversion (seen in the plots as a zone of sharp flow gradients). Typically collocated with the capping inversion layer is the so-called entrainment zone, through which the strongly turbulent CBL flow interacts with the relatively quiescent free-atmospheric flow aloft. Another characteristic feature of the CBL flow is its coherent structure on larger scales that is represented by convective updrafts (thermals) and downdrafts which are clearly observed in the vertical velocity field pattern (see Figure 4). This is also a clear indication of positive vertical skewness.

3 Experimental configurations

3.1 LES-based virtual radar

The method used to emulate the virtual radar signal within the atmospheric flow fields generated by LES is described by SCIPION et al. (2008) and is based on the work of MUSCHINSKI et al. (1999). The time-series data for the virtual BLR are created by summing the contribution from each LES point within the radar resolution volume which is defined by the radar pulse width and beam width. For this study, the virtual radar is patterned after a Vaisala UHF BLR-LAP3000 operating at a central frequency of 915 MHz, with a two-way half-power beam width of 9° . It is possible to direct the radar beam vertically or electronically steer it at 15.5° off-vertical along 4 different azimuth angles: 0° , 90° , 180° , 270° .

In the present study, a range resolution of 60 m is used to emulate the SGP ACRF parameters (see below). Additive white Gaussian noise, corresponding to a signal-to-noise ratio (SNR) of 10 dB, was added to the time-series data to produce more realistic signals. The three spectral moments (power, mean radial velocity, and spectral width) are estimated after conventional spectral analysis of the time-series data. The maximum time period for which data were processed for this case was ~ 11.5 hr. Radial velocities were later used to estimate the wind components using DBS, profiles of vertical velocity variance (second-order turbulence), and

profiles of vertical velocity skewness (third-order turbulence). Turbulence kinetic energy (eddy) dissipation rate (ϵ) estimates were obtained from the Doppler spectral width of the vertical beam after removal of beam broadening effects. The mean wind and turbulence parameters estimation algorithms based on virtual radar are validated with the LES “ground-truth”.

3.2 ARM Profiler field experiment

The 915 MHz radar wind profiler/radio acoustic sounding system (RWP/RASS) located at the SGP ACRF site provides wind profiles and backscattered signal strength in the height range of 0.1 km to 5 km (nominally) and sonic temperature profiles from 0.1 km to 2.5 km.

The radar typically operates in two modes with different range resolutions. The low-mode has a range resolution of 62.50 m and a maximum range of 2600 m, while the high-mode has a 212.55 m resolution and a maximum range of 6670 m. The radar has a 9° beam width and points in the four cardinal directions with a zenith angle of 15.5° . The dwell time in each mode during the observation period considered here was approximately 30 s while the revisit time was between 6 and 7 min. Only the low-mode is considered in this study. The three spectral moments are calculated based on the Doppler wind spectra downloaded from the ARM website.

4 Results

4.1 Mean wind field

For each of the three wind components (u , v , and w), three quantities were analyzed: DBS values calculated from the radial velocities of the virtual BLR pointing in the five directions (RadSim_{DBS}), resolved LES values along a vertical profile at the center the simulation domain (LES), and DBS estimates from the SGP ACRF radar (Radar_{ARM}). Based on the revisit time of the 915 MHz radar located at the SGP ACRF site, wind estimates were retrieved every 12 minutes. In order to provide a fair comparison between the three quantities, the averaging time for RadSim_{DBS} and LES velocities was also chosen to be 12 min.

To obtain the RadSim_{DBS} values, the following procedure was used. First, radial velocities from each of the five virtual BLR beams were estimated with a dwell time of 30 s. Second, velocity samples were computed every 6 min, approximately corresponding to the revisit time within one DBS cycle of the SGP ACRF measurements. Third, the velocities were averaged over 12-min periods representing the DBS sampling time. Finally, the DBS technique was used to retrieve the three wind components. The LES data were averaged in time to obtain 12-min estimates used for comparison. Radial velocities from Radar_{ARM} were averaged over the same time period, and values with $\text{SNR} \leq -10$ dB were censored for further analysis.

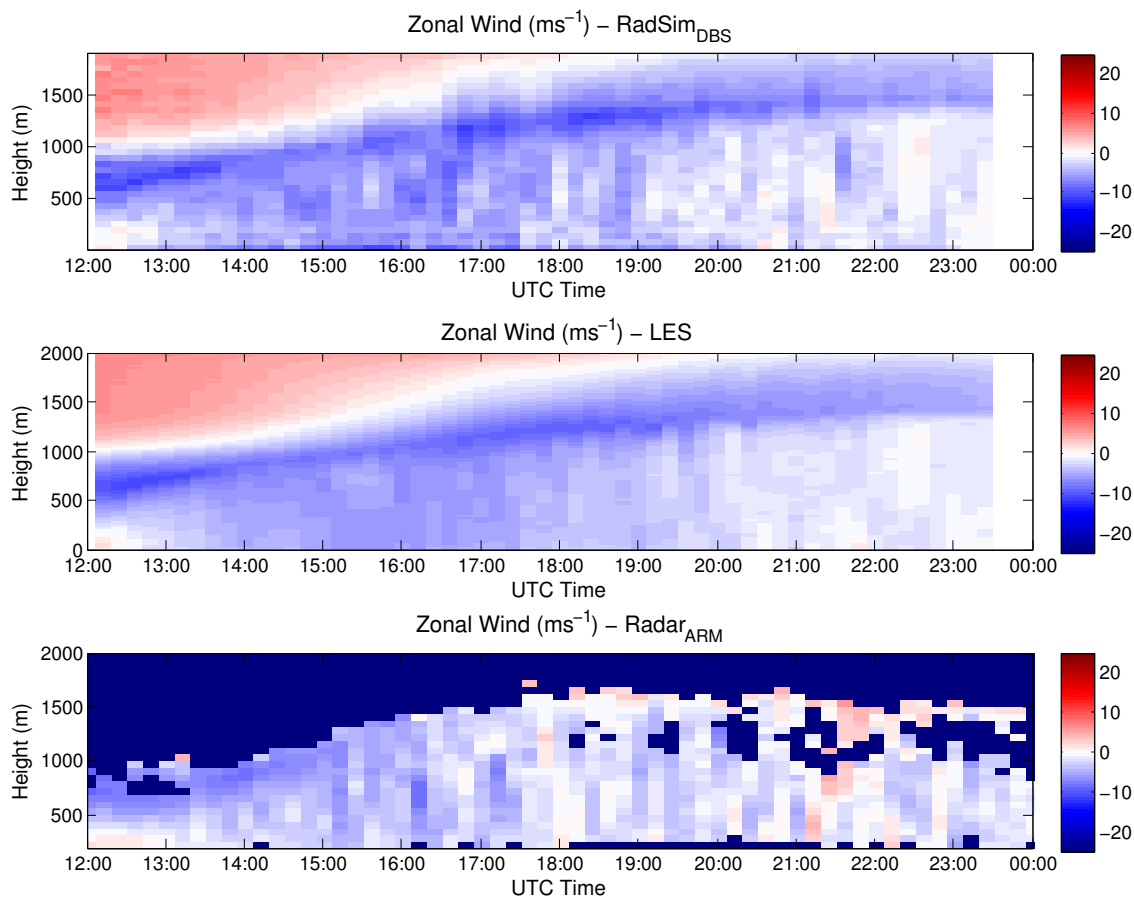


Figure 2: Zonal wind estimates averaged every 12 min on June 8 2007. Top: LES-DBS. Middle: LES-Profile at center of domain. Bottom: DBS estimates from the SGP ACRF radar.

Values of the three wind components obtained by different techniques are presented in Figures 2 (zonal), 3 (meridional), and 4 (vertical). The RadSim_{DBS} estimates do not appear as smooth as those from LES, primarily due to the realistic noise contamination and associated measurement error. In general, the wind fields retrieved from LES of the fair CBL case (in terms of the classification applied in BOTNICK and FEDOROVICH (2008)) agree well with the Radar_{ARM} estimates. Discrepancies observed (especially, in the zonal and vertical winds) apparently result from the evolution of external atmospheric forcing unaccounted for this version of the LES code. The LES was initialized using data from a rawinsonde launched at 11:30 UTC at the SGP ACRF site. The background atmospheric state represented by this initial sounding was assumed to be steady throughout the simulation. Therefore, evolution of turbulence fields within CBL was entirely determined by the surface heating, which was reproduced realistically based on data from surface heat balance measurements at the SGP ACRF site, and the variable geostrophic forcing. The agreement observed between the LES and the Radar_{ARM} reflects the ability of the LES code to reproduce, to a certain extent, the basic properties of the

evolving CBL flow fields. The good agreement between the RadSim_{DBS} and Radar_{ARM} demonstrates how the virtual BLR is able to reproduce these fields in a similar way as the real radar.

To quantify the wind parameters, two cross-sectional cuts were made in the wind component fields referring to the elevations ~ 530 m and ~ 1030 m. Wind component estimates for all three sources are presented in Figure 5 together with corresponding sounding data at 12:00, 18:00, and 00:00 UTC. There is a general agreement between the estimates from RadSim_{DBS}, LES, and the sounding data for both heights and at all times. The agreement between the estimates from the LES and Radar_{ARM} is especially good for low elevations. There are some discrepancies at higher altitudes partially due to low SNR at particular time intervals.

Another cause for discrepancies in the estimates is the apparent inability of the LES code in its current version to account for the evolution of environmental (larger-scale) forcing, whose contribution at certain stages of the CBL evolution is comparable to the effects of simulated surface and shear forcing. This makes the pace of the CBL growth in the LES more gradual than was observed at the SGP ACRF site and reproduced by the local

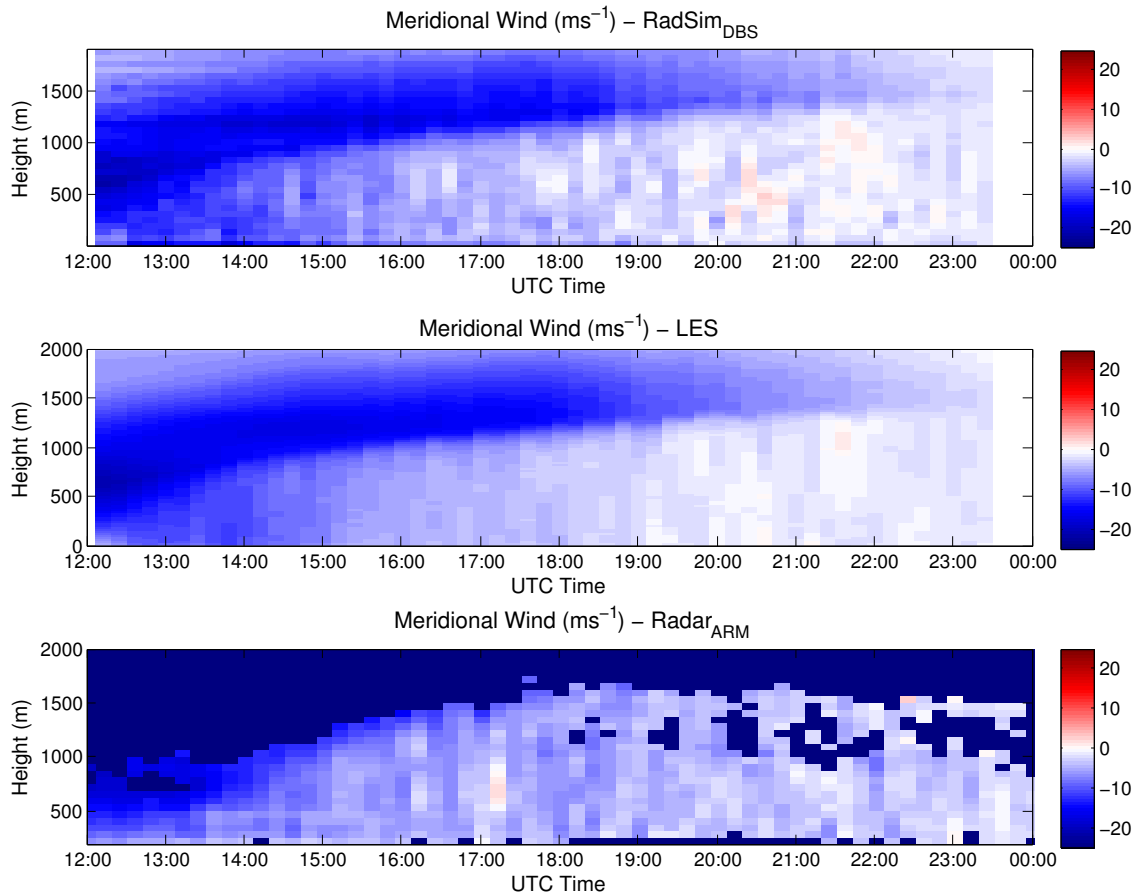


Figure 3: Meridional wind estimates averaged every 12 min on June 8 2007. Top: LES-DBS. Middle: LES-Profile at center of domain. Bottom: DBS estimates from the SGP ACRF radar.

radar. For instance, wind field estimates around 1030 m correspond to different CBL regions: in the Radar_{ARM} this elevation is within the mixing layer, while for the LES and RadSim_{DBS}, the estimated wind refers to an elevation with two different CBL regions: before 15:45, the free atmosphere above the CBL top, and after 15:45, the mixing layer inside the CBL. The estimations of the different regions for the LES and RadSim_{DBS} are obtained based on the structure function parameter of refractivity (C_n^2) obtained from the LES parameters following the procedure described in SCIPION et al. (2008), and for the Radar_{ARM} from the range corrected SNR. An adjustment of the LES fields to the evolving environmental atmospheric conditions will be realized as a part of future work, as described in Section 5.

4.2 Vertical velocity variance

The values of vertical velocity w obtained by all three techniques are used to estimate the vertical variance of w . With regard to the LES, this procedure involves estimating the fluctuating component of the vertical velocity (w') from the time series of the resolved w field retrieved from the LES output for a particular location (center of

the LES domain). To account for the effect of sub-grid turbulence, a sub-grid component of variance is added to the resolved variance (Eq. 4.1). This component is represented (assuming isotropy of the sub-grid turbulence) by two thirds of the time-averaged values of the sub-grid turbulence kinetic energy. That is,

$$\sigma_w^2(LES) = \overline{w'w'} + \frac{2}{3}\overline{E}, \quad (4.1)$$

$$\sigma_w^2(Radar) = \overline{w'w'}, \quad (4.2)$$

where w' and E are the vertical velocity fluctuation and sub-grid kinetic energy, respectively. The over-bar represents the time average. Before calculating the deviation from the mean, a linear de-trending procedure is performed for all the vertical wind estimates (ANGEVINE et al., 1994). Estimates of the vertical velocity variances from RadSim, LES, and Radar_{ARM} for the CBL case of June 8, 2007 applying an averaging time of two hours for different periods of time (14:00–16:00; 16:00–18:00; 18:00–20:00; and 20:00–22:00 UTC) are presented in Fig. 6. The CBL top is also presented in the same Figure as a horizontal dashed line at each of the averaged periods as reference. This rudimentary es-

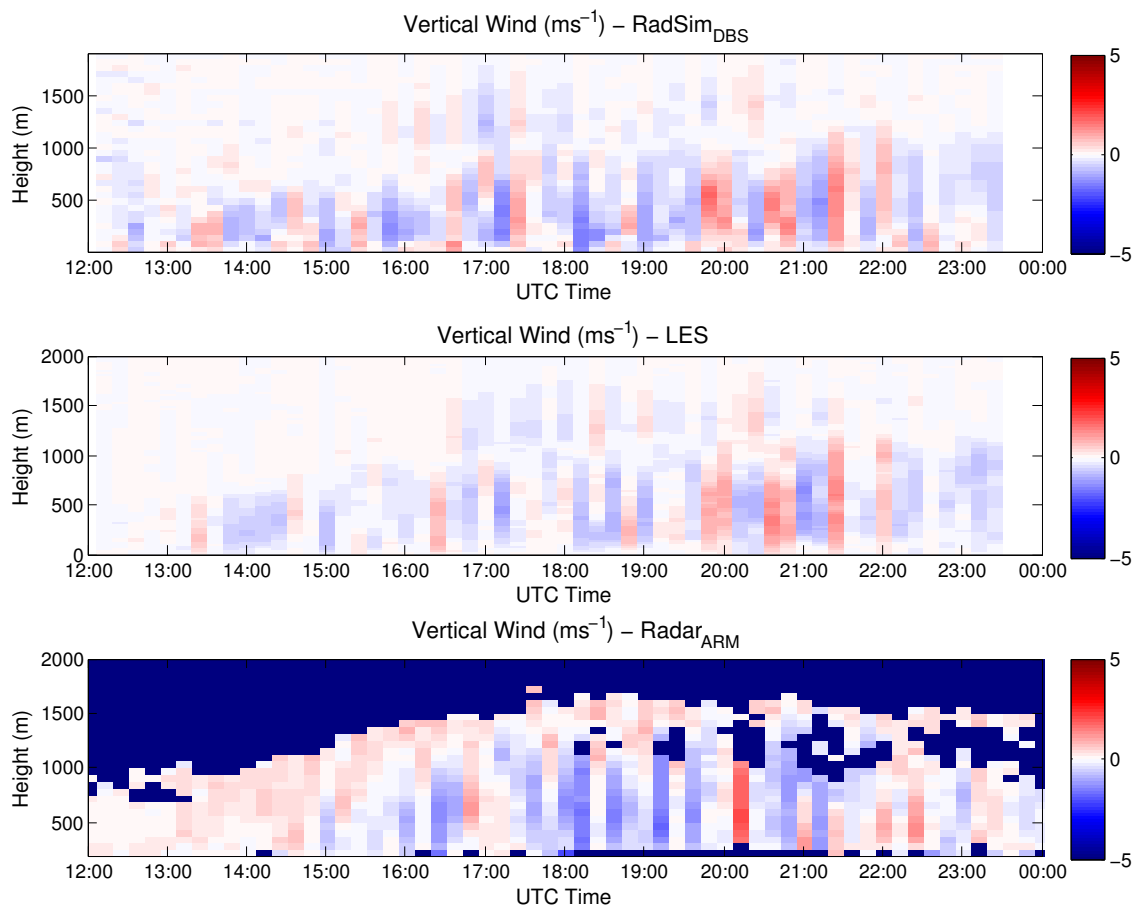


Figure 4: Vertical wind estimates averaged every 12 min on June 8, 2007. Top: LES-DBS. Middle: LES-Profile at center of domain. Bottom: DBS estimates from the SGP ACRF radar.

estimate of the CBL top is taken from the maximum of C_n^2 . The CBL/inversion layer top estimated is located at 850 m, 1050 m, 1100 m, and 1250 m, for each averaged period respectively. The LES w field, considered as a reference data source, and RadSim vertical velocity are sampled every 6 min to emulate the revisit time of the Radar_{ARM}. The averaging and sampling times used clearly filter the high frequency components of the variance, especially for LES. However, as mentioned before, their use is justified to obtain realistic comparisons with the SGP ACRF data.

The decrease in the vertical velocity variance observed (especially noticeable in the RadSim profiles) is a clear indication of the CBL/inversion layer top. As can be seen in the plot, the drop in variance corresponds roughly to the upper boundary of the CBL and the height of this feature increases over time as the CBL continues to develop. For the four periods, the minimum is observed at around 850 m, 1050 m, 1100 m, and 1250 m, for the 14:00-16:00; 16:00-18:00; 18:00-20:00; and 20:00-22:00 UTC period, respectively. These results are in excellent agreement with the estimates obtained as reference from C_n^2 . The discrepancy between the RadSim and the LES estimates may be due in part

to the sub-grid kinetic energy contribution, which is not accounted for in the radar simulator and to the noise, which was added to the simulated time-series data. The primary cause of discrepancies in the w variance profile shapes from the LES and Radar_{ARM} estimates is attributed to the aforementioned inconsistency of prediction of the CBL depth evolution associated with external forcings.

4.3 Vertical velocity skewness

The skewness of the vertical velocity (w) in the CBL is a signature feature of the CBL flow structure (MOENG and ROTUNNO, 1990):

$$skewness = \frac{\overline{w'w'w'}}{(\overline{w'w'})^{\frac{3}{2}}}. \quad (4.3)$$

Positive w skewness throughout the main portion of the CBL is indicative of localized and intense upward vertical motions (updrafts) as compared to relatively widespread and gentle downward motions (downdrafts) (see Figure 4). The height dependence of the vertical velocity skewness in the CBL has been previously

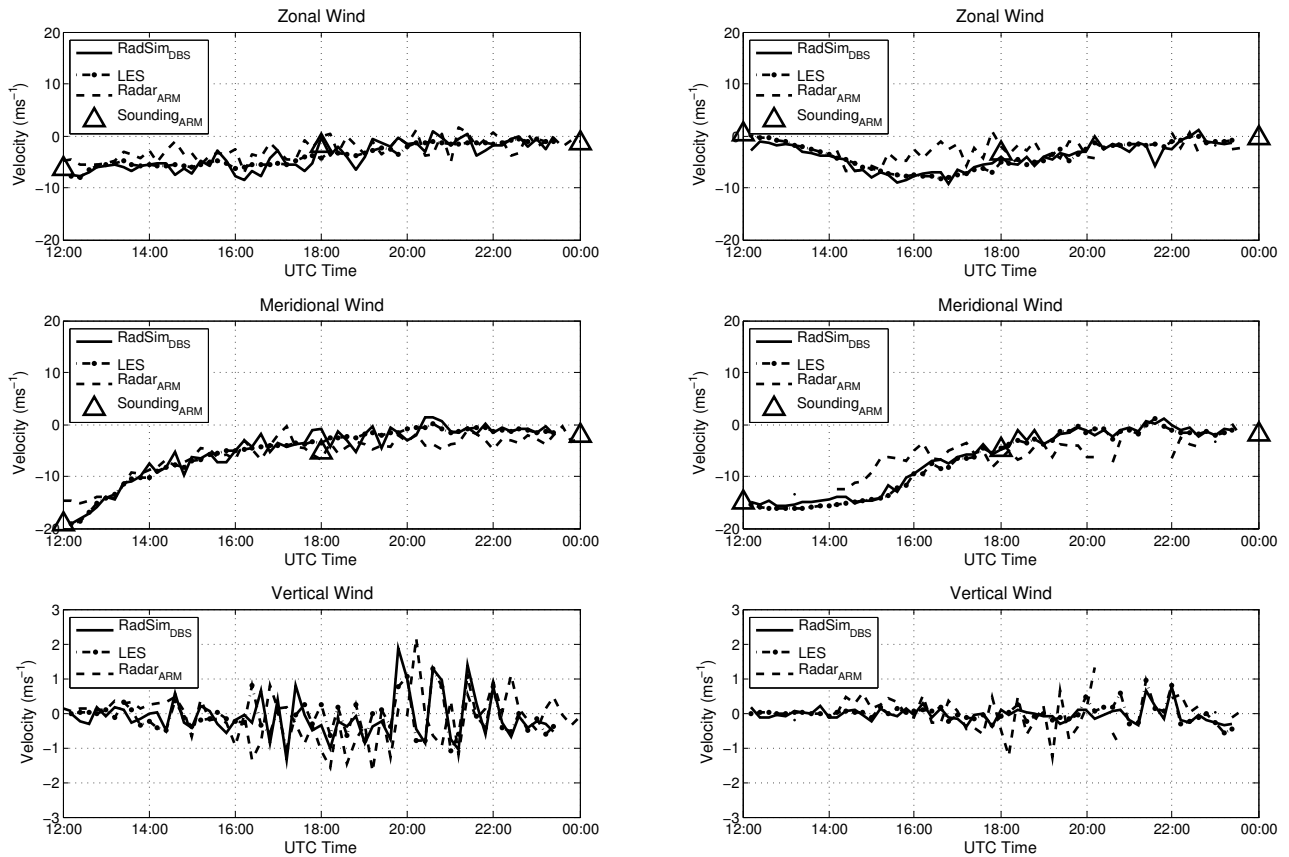


Figure 5: Wind comparison from the RadSim_{DBS}, LES, Radar_{ARM}, and a sounding (launched at three different times: 12:00, 18:00, and 00:00 UTC) at ~530 m (left) and ~1030 m (right) on June 8, 2007. Top: zonal wind. Middle: meridional wind. Bottom: vertical velocity.

analyzed using LES in conjunction with observations (MOENG and ROTUNNO, 1990) and LES in conjunction with wind tunnel measurements (FEDOROVICH et al., 1996, 2001). As mentioned before, the sampling period chosen filters the high frequency components of the spectrum and skewness as well, but is the most appropriate for comparisons with real data. Here, we calculate vertical profiles of skewness using vertical velocity data from RadSim, LES, and Radar_{ARM} for the CBL case of June 8, 2007 applying an averaging time of two hours for different stages of the CBL evolution (14:00–16:00; 16:00–18:00; 18:00–20:00; and 20:00–22:00 UTC). The vertical velocity fields from LES and RadSim are sampled every 6 min to reproduce the revisit time of the Radar_{ARM}. The results are presented in Figure 7 for comparison. Note that the estimates of skewness from all three sources exhibit similar behavior. That is, within the main portion of the CBL, the values are found to be positive. This is consistent with the large-scale pattern in the vertical velocity, characteristic of the mixed-layer. Skewness increases in magnitude and range of positive values of w toward the CBL top; this growth can be clearly identified at each time period.

In the simulated CBL, the skewness reaches a maximum around the base of the inversion, and then drops

to zero in the interior of the inversion layer, where the upward component of turbulent motion is in approximate equilibrium with the downward component (FEDOROVICH et al., 2001). From 14:00 to 16:00, the increase in skewness is observed around 600 m, reaching the top of inversion layer at around 750 m. In this period, the skewness estimates are rather inconsistent and, as a consequence, the estimate of the CBL top based on the skewness profile appears to be unreliable. For the other time periods (16:00–18:00; 18:00–20:00; and 20:00–22:00) the maximum in skewness occurs at 900 m, 950 m, and 1100 m; and the CBL/inversion layer top estimated from vertical velocity variance and the maximum of C_n^2 is located at 1050 m, 1100 m, and 1250 m, respectively. Coincidentally, the difference between the estimates from the vertical velocity variance and the maximum in skewness is 150 m. Radar estimates of skewness agree well with the LES estimates and are similar to those presented in FEDOROVICH et al. (1996, 2001). While analyzing the obtained skewness profile one should keep in mind that skewness is very sensitive to the sample size, which in the reported retrieval procedures was rather small due to the necessity of bringing data from all sources to one sampling time window corresponding to the radar revisit time (see above).

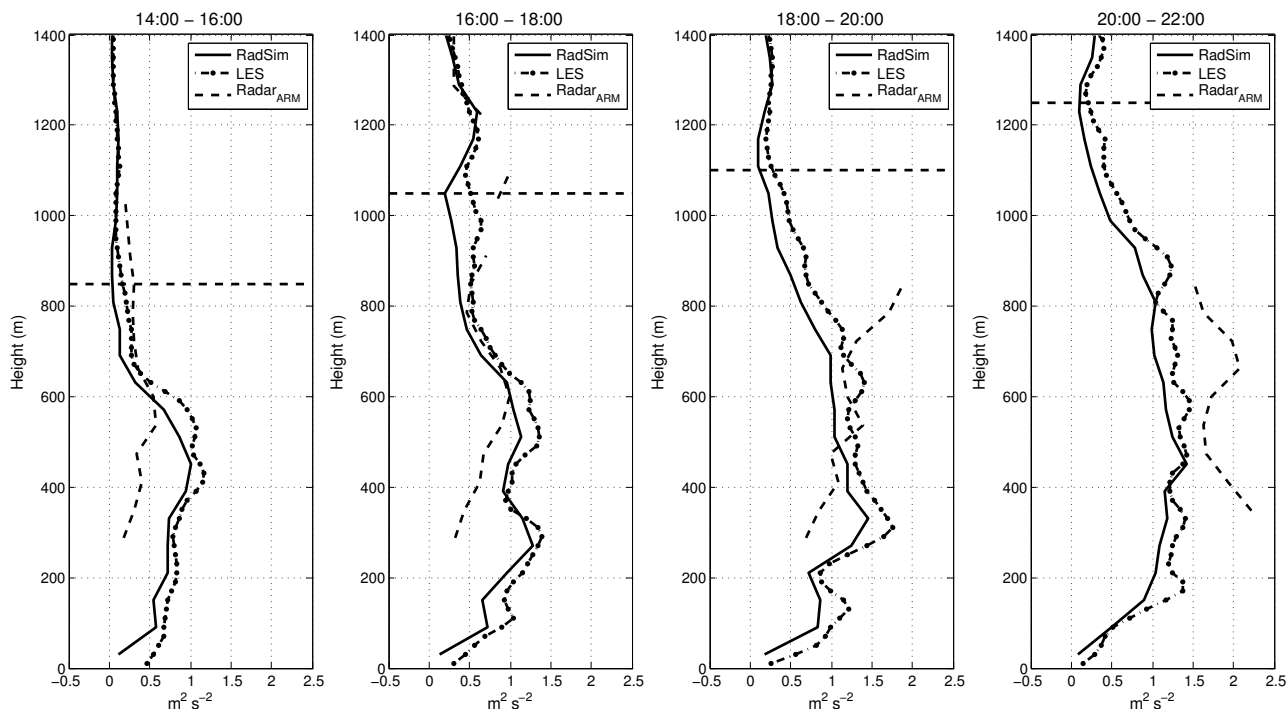


Figure 6: Vertical velocity variance as a function of height for different periods of time from left to right (14:00-16:00; 16:00-18:00; 18:00-20:00; and 20:00-22:00 UTC). Continuous line: estimates from the virtual BLR. Dot-dashed: estimates from the LES. Dashed line: estimates from the BLR located at the SGP ACRF site. The horizontal dashed line represents the CBL top obtained from the LES C_n^2 maximum averaged over the period under study.

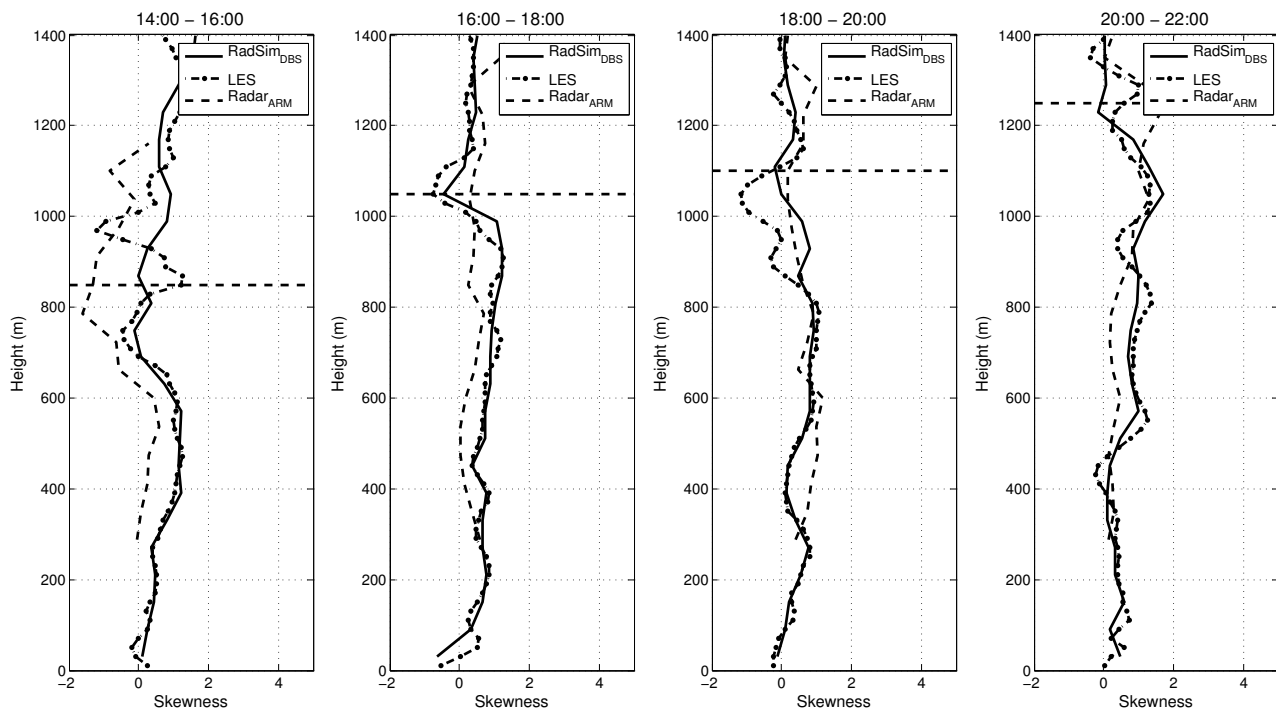


Figure 7: Skewness of the vertical velocity as a function of height for different periods of time from left to right (14:00-16:00; 16:00-18:00; 18:00-20:00; and 20:00-22:00 UTC). Continuous line: estimates from the virtual BLR. Dot-dashed line: estimates from the LES. Dashed line: estimates from the BLR located at the SGP ACRF site. The horizontal dashed line represents the CBL top obtained from the LES C_n^2 maximum averaged over the period under study.

4.4 Estimates of dissipation from Doppler spectral width

An increase in the Doppler spectral width for radar measurements is due to spatial and temporal variations of radial velocities within the radar resolution volume. Contributions to the spectral width (σ_v), according to WHITE (1997); JACOBY-KOALY et al. (2002), result from velocity fluctuations with scales smaller than the radar resolution volume (broadening due to turbulence σ_{11}), velocity fluctuations with scales larger than the radar resolution volume (shear broadening due to larger-scale variations of wind fields σ_s), and other contributions that can be attributed to the specifics of the signal processing scheme (σ_x). DOVIAK and ZRNIC (1984) show that the Doppler spectral width is related to the individual contributions via:

$$\sigma_v^2 = \sigma_{11}^2 + \sigma_s^2 + \sigma_x^2. \quad (4.4)$$

Other spectrum broadening effects identified by previous studies (HOCKING, 1983, 1985; NASTROM and EATON, 1997) include specular reflections from stable layers (especially along the vertical beam), gravity waves, or water particles (BLRs are also sensitive to Rayleigh scatters). These cases correspond to different types of scattering processes that are not directly relevant to the present study in the CBL.

Contributions from the shear broadening effect have been studied extensively (i.e., DOVIAK and ZRNIC, 1984; GOSSARD, 1990; WHITE, 1997; JACOBY-KOALY et al., 2002). The term σ_s^2 in the above equation can be decomposed into a beam broadening component (this is only a function of the beam-width and of the horizontal wind velocity) and into a variance component involving terms due to wind shear. Depending on the pointing angle, either can be more representative. For a vertically pointing beam, shear broadening is dominated by the beam broadening effect as described by WHITE (1997); JACOBY-KOALY et al. (2002):

$$\sigma_s^2 = \frac{\theta_1^2}{12 \ln 2} V_H^2, \quad (4.5)$$

where θ_1 represents the two-way, 3 dB radar beam-width, and V_H the horizontal wind magnitude.

The signal processing contribution (σ_x^2) depends on many factors. These include pointing direction, low SNR, ground-clutter removal, etc. Bias in the spectral width estimate related to low SNR is not analyzed here, as the Radar_{ARM} data were censored for low SNR values and the SNR considered in RadSim is set to 10 dB. In the case of spectra retrieved from a vertically pointing beam, the mean velocity or first moment is in many cases close to, or partly embedded in, the ground-clutter region. In this study we focus on one of the principal signal processing contributions associated with finiteness of time series, the so-called windowing effect. It tends to broaden the estimated spectra. The windowing effect

is the only signal processing effect considered in this report. Its contribution is constant and it is calculated from the Fourier transform of the window (3-dB spectral width). When turbulence is weak (especially above the CBL or during the night), the removal of the contributions can lead to negative values of σ_{11}^2 . WHITE (1997); WHITE et al. (1999); JACOBY-KOALY et al. (2002) neglected any negative values of σ_{11}^2 .

With the assumptions of homogeneity and isotropy, and assuming that the beam weighting function, as well as the range weighting function are Gaussian, the turbulence variance σ_{11}^2 is related to the turbulence kinetic (eddy) dissipation rate ϵ by equation (5.32) from WHITE (1997). After converting to spherical coordinates and approximating $\text{sinc}^2(x)$ with $\exp(-x^2/3)$ (the approximation has a margin of error of 2 %), WHITE et al. (1999) obtained a more manageable expression for the eddy dissipation rate (ϵ):

$$\epsilon = \sigma_{11}^3 (4\pi/A)^{3/2} J^{-3/2} \quad (4.6)$$

$$J = 12\Gamma(2/3) \int_0^{\pi/2} (\sin^3 \varphi) (b^2 \cos^2 \varphi + a^2 \sin^2 \varphi + (L^2/12) \sin^2 \varphi \cos^2 \varphi)^{1/3} d\varphi \quad (4.7)$$

$$L = V_T t_D \quad (4.8)$$

$$a = \frac{R\theta_1}{2\sqrt{2 \ln 2}} \quad (4.9)$$

$$b = 0.3\Delta R, \quad (4.10)$$

where Γ is the Gamma function, V_T is the wind speed transverse to the radar beam, t_D is the radar dwell-time (WHITE, 1997), and a and b are related to the inverse of the two-way variance of the Gaussian beam weighting function and Gaussian range weighting function, respectively. The parameter $A = 1.6$ represents the empirical Kolmogorov constant in the inertial subrange of the velocity spectrum. Finally, R and ΔR represent the center of the range gate and range spacing, respectively. Note that ϵ is proportional to the cube of σ_{11} . This implies that the turbulence dissipation rate is quite sensitive to variations of σ_{11} .

The resulting ϵ values retrieved from the Doppler spectral width for both virtual and actual BLRs are compared against the LES dissipation estimates. In this study, the LES ϵ is obtained from the parametrized expression for the dissipation rate that enters the prognostic equation for the sub-grid (residual) kinetic energy solved in the employed LES (POPE, 2000). Eddy dissipation rate profiles of the RadSim_{DBS}, LES, and Radar_{ARM} are averaged in periods of two hours (14:00–16:00; 16:00–18:00; 18:00–20:00; 20:00–22:00 UTC) and are presented in Figure 8.

The three estimates seem to have the same behavior in most parts of the mixing-layer, however near the inversion layer the radar estimates start to deviate from

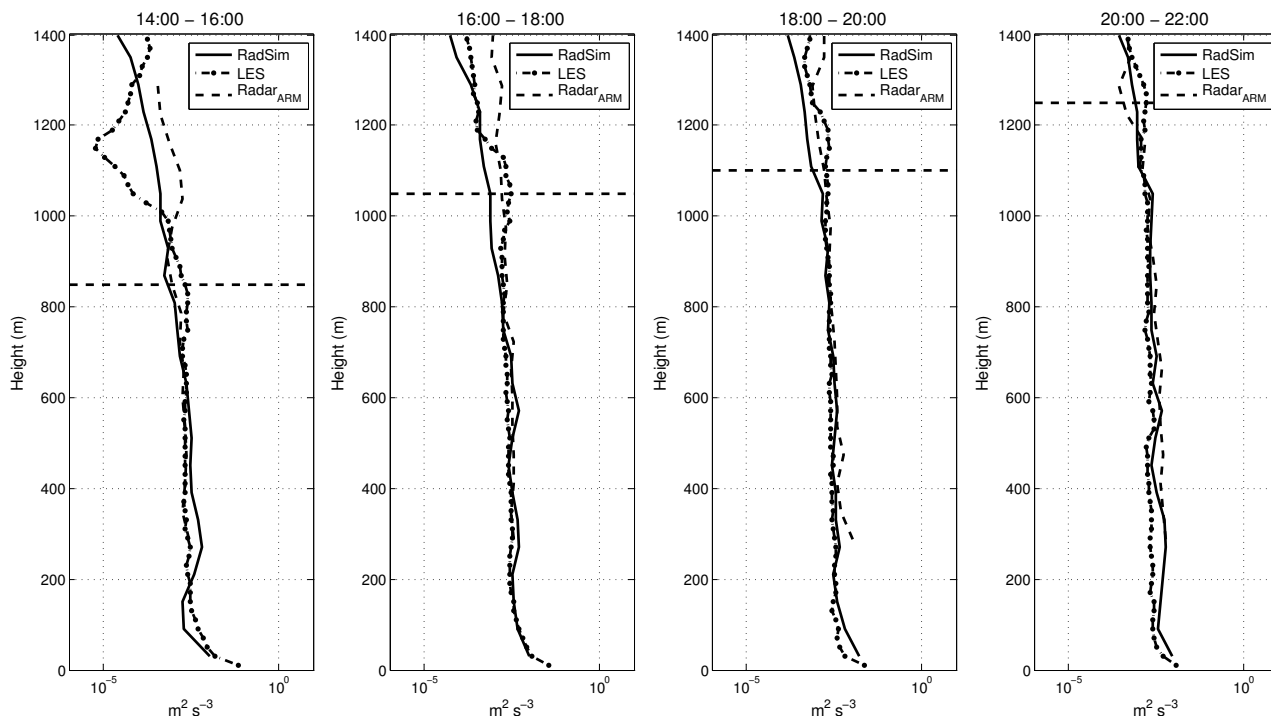


Figure 8: Turbulence eddy dissipation rate average profiles for different periods of time from left to right (14:00–16:00; 16:00–18:00; 18:00–20:00; and 20:00–22:00 UTC). Continuous line: estimates from the virtual BLR spectral width. Dot-dashed line: estimates from the LES. Dashed line: estimates from the BLR located at the SGP ACRF site. The horizontal dashed line represents the CBL top obtained from the LES C_n^2 maximum averaged over the period under study.

the LES profile. Above the inversion layer, the spectral width estimates are not reliable because the turbulence is weak and residual noise contribution is unquantifiable. Dissipation profiles in Figure 8 provide close estimates of the CBL upper interface elevations within the considered time intervals. These estimates can be identified clearly in the Figure as the point where a sharp decrease in the LES profile starts. This point is located at 1000 m, 1200 m, 1250 m, and 1400 m, for 14:00–16:00; 16:00–18:00; 18:00–20:00; 20:00–22:00 UTC periods, respectively. Once again, the CBL top has been previously identified from the velocity variance and maximum of C_n^2 to be around 850 m, 1050 m, 1100 m, and 1250 m for each of the time intervals; and there is a constant separation of 150 m between CBL top and upper interface estimates. This agreement shows once more the potential of radar measurements of the CBL.

5 Conclusions and future work

Comparisons of the virtual BLR radial velocities with LES velocity estimates have been presented. The LES output has also been compared with actual radar data for the CBL case observed on the U.S. Central Plains on June 8, 2007. Reasonable quantitative agreement was found in the zonal, meridional, and vertical wind fields retrieved from the radar and estimated from LES. This

agreement reflects the ability of the employed LES code to reproduce basic properties of the CBL mean flow for the studied case. Estimates of the mean wind by virtual (RadSim) and real (Radar_{ARM}) radars are also in good agreement, indicating that the virtual BLR (Scipi3n et al., 2008) is capable of reliable characterization of atmospheric flow in a similar way as the real radar.

Estimates of the vertical velocity variance from LES and RadSim are generally in good agreement. The small discrepancies between the estimates are apparently due to the effects of sub-grid turbulence unaccounted by the radar simulator. The differences between the LES and Radar_{ARM} variances may be attributed to the inability of LES to sufficiently reproduce the actual evolution of the CBL depth, particularly during the morning stages. The sharp decrease in the vertical velocity variance in the upper portion of the CBL can be used as a rough indicator of the top of the capping inversion layer and of the overall CBL top. This decrease is clearly observed in the variance data retrieved from LES and virtual radar for subsequent stages of CBL growth.

The skewness of the vertical velocity has been analyzed as a function of height. In the well-mixed portion of the CBL, skewness estimates are essentially positive and their magnitude increases with height in agreement with MOENG and ROTUNNO (1990). The estimates from the three sources agree well, especially

within the well-mixed portion of the CBL. The estimates of CBL depth from skewness profiles demonstrate fair agreement with those retrieved from vertical velocity variance distributions.

The broadening of the Doppler spectrum resulting from turbulence within the radar resolution volume has been estimated using the procedure outlined in WHITE (1997). These estimates were used to compute the turbulence kinetic energy (eddy) dissipation rate. The eddy dissipation rate profiles from the virtual and actual radars have been evaluated against eddy dissipation data from the LES and have demonstrated generally good agreement with numerical results, especially within the mixing layer. The discrepancies observed above the capping inversion layer were presumably caused by weak turbulence and/or the presence of residual noise that had not been removed.

Further work is planned in order to focus on evaluating flow homogeneity assumptions for wind velocity calculations using DBS. In the presence of inhomogeneities, DBS estimates are not always reliable, especially if the time needed to complete a DBS scan is large, on the order of a few minutes. In the anticipated study, LES output will be analyzed in conjunction with three-dimensional wind estimates obtained from DBS and Spaced Antenna (SA). The latter technique incorporates a vertical beam for transmission, and the backscattered signal is received using spatially separated antennas. As a result, the SA technique should rely less heavily on the spacial homogeneity requirement as compared to the DBS technique. However, shear in the vertical velocity field may play a large role in the reliability of these estimates and will be studied in future work.

As indicated in BOTNICK and FEDOROVICH (2008), the CBL case of June 8, 2007 is one of the cases for which the LES predictions compare rather favorably with sounding data (see Figure 5). To make the employed LES code capable of reproducing a wider range of CBL conditions associated with different environmental forcing, further work will include the implementation of a new numerical procedure providing adjustment (nudging) of the simulated CBL mean flow fields to evolving larger scale external flow fields retrieved from either observational or numerical model data. The nudging procedure will be realized by adding time-tendency terms to the prognostic equations for filtered (resolved), in the LES sense, horizontal momentum, potential temperature, and humidity fields. These terms could be taken as proportional to the difference between the horizontally averaged LES fields and profiles of the corresponding environmental variables. They are intended to act in a force-restoring manner by preventing LES fields from deviating too much, on average, from the environmental flow throughout the LES domain. The optimal value of the restoring time constant will be found through a series of numerical experiments.

The promising agreement of wind retrievals and second-, and third- order statistics from LES, virtual

radar, and real radar encourages us to continue our research to further characterize the CBL wind and turbulent fields through a combination of both techniques.

Acknowledgments

The authors of this work acknowledge the National Science Foundation (NSF) for their support via grant ATM-0553345. Observational data for this study were obtained from the Atmospheric Radiation Measurement (ARM) Program sponsored by the U.S. Department of Energy, Office of Science, Office of Biological and Environmental Research, Environmental Science Division.

References

- ANGEVINE, W.M., R.J. DOVIK, Z. SORBJAN, 1994: Remote Sensing of Vertical Variance and Surface Heat Flux in a Convective Boundary Layer. – *J. Appl. Meteorol.* **33**, 977–983.
- BALSLEY, B.B., K. GAGE, 1982: On the use of radars for operational profiling. – *Bull. Amer. Meteor. Soc.* **63**, 1009–1018.
- BOTNICK, A.M., E. FEDOROVICH, 2008: Large eddy simulation of atmospheric convective boundary layer with realistic environmental forcings. – In: MEYERS, J. et al. (Eds.): *Quality and Reliability of Large-Eddy Simulations*, Springer, 193–204.
- COHN, S.A., 1995: Radar measurements of turbulent eddy dissipation rate in the troposphere: A comparison of techniques. – *J. Atmos. Oceanic Technol.* **12**, 85–95.
- CONZEMIUS, R.J., E. FEDOROVICH, 2006: Dynamics of sheared convective boundary layer entrainment. Part I: Meteorological background and large-eddy simulations. – *J. Atmos. Sci.* **63**, 1151–1178.
- DOVIK, R., D.S. ZRNIC, 1984: Reflection and scatter formula for anisotropically turbulent air. – *Radio Sci.* **19**, 325–336.
- DURRAN, D.R., 1999: *Numerical methods for wave equations in geophysical fluid dynamics*. – Springer-Verlag New York, Inc.
- FEDOROVICH, E., R. CONZEMIUS, 2008: Effects of wind shear on the atmospheric convective boundary layer structure and evolution. – *Acta Geophysica* **56**, 114 – 141.
- FEDOROVICH, E., R. KAISER, M. RAU, E. PLATE, 1996: Wind Tunnel Study of Turbulent Flow Structure in the Convective Boundary Layer Capped by Temperature Inversion. – *J. Atmos. Sci.* **53**, 1273–1289.
- FEDOROVICH, E., F.T.M. NIEUWSTADT, R. KAISER, 2001: Numerical and laboratory study of horizontally evolving convective boundary layer. Part I: Transition regimes and development of the mixed layer. – *J. Atmos. Sci.* **58**, 70–86.
- FEDOROVICH, E., R. CONZEMIUS, I. ESAU, F.K. CHOW, D. LEWELLEN, C.-H. MOENG, D. PINO, P. SULLIVAN, J.V.-G. DE ARELLANO, 2004a: Entrainment into sheared convective boundary layers as predicted by different large eddy simulation codes. – Preprints, 16th Symp. on Boundary Layers and Turbulence, Amer. Meteor. Soc., 9-13 August, Portland, Maine, USA CD-ROM, P4.7.
- FEDOROVICH, E., R. CONZEMIUS, D. MIRONOV, 2004b: Convective entrainment into a shear-free linearly stratified atmosphere: Bulk models re-evaluated through large-eddy simulations. – *J. Atmos. Sci.* **61**, 281–295.

- GOSSARD, E.E., 1990: Radar research on the atmospheric boundary layer. – In: ATLAS D. (Ed.): Radar in Meteorology, Amer. Meteor. Soc., Boston, Mass., 477–527.
- GOSSARD, E.E., D.C. WELSH, R.G. STRAUCH, 1990: Radar-measured height profiles of C_n^2 and turbulence dissipation rate compared with radiosonde data during October 1989 at Denver. – NOAA Technical Report ERL 442-WPL 63276, Environmental Research Laboratories.
- GOSSARD, E.E., D.E. WOLFE, K.P. MORAN, R.A. PAULUS, K.D. ANDERSON, L.T. ROGERS, 1998: Measurement of clear-air gradients and turbulence properties with radar wind profilers. – *J. Atmos. Oceanic Technol.* **15**, 321–342.
- HOCKING, W.K., 1983: On the extraction of atmospheric turbulence parameters from radar backscatter Doppler spectra, part I; Theory. – *J. Atmos. Terr. Phys.* **45**, 89–102.
- 1985: Measurement of turbulent eddy dissipation rates in the middle atmosphere by radar techniques: A review. – *Radio Sci.* **20**, 1403–1422.
- 1996: An assessment of the capabilities and limitations of radars in measurements of Upper Atmospheric turbulence. – *Adv. Space Res.* **17**, 37–47.
- JACOBY-KOALY, S., B. CAMPISTRON, S. BERNARD, B. BÉNECH, F. ARDHUIN-GIRARD, J. DESSENS, E. DUPONT, B. CARISSIMO, 2002: Turbulent dissipation rate in the boundary layer via UHF wind profiler Doppler spectral width measurements. – *Bound.-Layer Meteor.* **103**, 361–389.
- MOENG, C.-H., R. ROTUNNO, 1990: Vertical-Velocity Skewness in the Buoyancy-Driven Boundary Layer. – *J. Atmos. Sci.* **19**, 1149–1162.
- MUSCHINSKI, A.P., P.P. SULLIVAN, R.J. HILL, S.A. COHN, D.H. LENSCHOW, R.J. DOVIK, 1999: First synthesis of wind-profiler signal on the basis of large-eddy simulation data. – *Radio Sci.* **34**, 1437–1459.
- NASTROM, G.D., F.D. EATON, 1997: Turbulence Eddy Dissipation Rate from Radar Observations at 5–20 km at White Sands Missile Range, New Mexico. – *J. Geophys. Res.* **102**, 19,495–19,505.
- POPE, S.B., 2000: – Turbulent Flows. – Cambridge University Press.
- SCIPIÓN, D.E., R.D. PALMER, E. FEDOROVICH, P.B. CHILSON, A.M. BOTNICK, 2007: Structure of a Daytime Convective Boundary Layer Revealed by a Virtual Radar Based on Large Eddy Simulation. – 33rd Conference on Radar Meteorology American Meteorological Society, Cairns, Australia.
- SCIPIÓN, D.E., P.B. CHILSON, E. FEDOROVICH, R.D. PALMER, 2008: Evaluation of an LES-based Wind Profiler Simulator for Observations of a Daytime Atmospheric Convective Boundary Layer. – *J. Atmos. Oceanic Technol.* **25**, 1423–1436.
- SHAW, W.J., M.A. LEMONE, 2003: Turbulence dissipation rate measured by 915 Mhz wind profiling radars compared with in-situ tower and aircraft data. – 12th Symposium on Meteorological Observations and Instrumentations American Meteorological Society, California.
- SPIZZICHINO, A., 1975: Spectral broadening of acoustic and radio waves scattered by atmospheric turbulence in the case of radar and sodar experiments. – *Ann. Geophys.* **31**, 433–445.
- WHITE, A.B., 1997: Radar remote sensing of scalar and velocity microturbulence in the convective boundary layer. – NOAA Technical Memorandum ERL ETL-276, Environmental Research Laboratories.
- WHITE, A.B., R.J.A. LATAITIS, R.S. LAWRENCE, 1999: Space and time filtering of remotely sensed velocities turbulence. – *J. Atmos. Oceanic Technol.* **16**, 1967–1972.